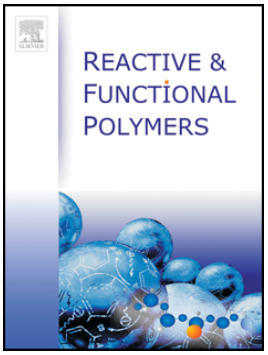

Preparation and characterization of novel side-chain azobenzene polymers containing tetrazole group

Xiaoqiang Xue, Jing Yang, Wenyan Huang, Hongjun Yang, Bibiao Jiang

PII: S1381-5148(15)30045-6
DOI: doi: 10.1016/j.reactfunctpolym.2015.09.007
Reference: REACT 3564

To appear in:

Received date: 30 April 2015
Revised date: 26 June 2015
Accepted date: 24 September 2015

Please cite this article as: Xiaoqiang Xue, Jing Yang, Wenyan Huang, Hongjun Yang, Bibiao Jiang, Preparation and characterization of novel side-chain azobenzene polymers containing tetrazole group, (2015), doi: 10.1016/j.reactfunctpolym.2015.09.007

Article type: Full Paper

Preparation and Characterization of Novel Side-Chain Azobenzene Polymers Containing Tetrazole Group

Xiaoqiang Xue, Jing Yang, Wenyan Huang, Hongjun Yang, Bibiao Jiang*

Jiangsu Key Laboratory of Material Surface Science and Technology, School of Material Science and Engineering, Changzhou University, Changzhou, Jiangsu, 213164, People's Republic of China

*Corresponding author. Tel.: 8651986330328;

E-mail: jiangbibiao@cczu.edu.cn

Abstract

A novel methacrylate monomer containing azobenzene chromophore and tetrazole moiety, 4′-(2-methacryloxyethyl)methylamino-4-(5-chlorotetrazol-1-yl)azobenzene (MACA), was synthesized and polymerized to form homopolymer (PMACA) via reversible addition-fragmentation chain transfer (RAFT) polymerization using 2-cyanoprop-2-yl dithiobenzoate (CPDB) as the RAFT agent and azobisisobutyronitrile (AIBN) as an initiator in dimethyl formamide (DMF) solution. Meanwhile, block copolymers (PMMA-*b*-PMACAs) were successfully obtained by RAFT polymerization of MACA using PMMA as the macro-RAFT agent and AIBN as an initiator. Gel permeation chromatography (GPC) characterization indicated that polymers with well-controlled molecular weights and narrow molecular weight distributions (M_w/M_ns <1.30) were obtained. The structures of these polymers were characterized by ^{1}H NMR and FT-IR spectra. Thermal and photoisomerization behaviors of the polymers indicated that these polymers were amorphous state with good heat stability and photoisomeriztion performance. Relationship between the electrochemical behavior of block copolymer (PMMA-*b*-PMACA) and the photoisomerization of azobenzene was investigated by cyclic voltammetry (CV) in chloroform solution, which showed that the oxidation peak of copolymer shifted from 1.0V to 0.6V during azobenzene isomerization from *trans* to *cis* form. Furthermore, surface relief gratings (SRGs) formed on the films of PMMA-*b*-PMACAs were also investigated with illumination of a linearly polarized Kr^+ laser beam. The diffraction efficiency of the SRGs was 1.22 (PMMA-*b*-PMACA1), 2.38 (PMMA-*b*-PMACA2) and 3.02 (PMMA-*b*-PMACA3), respectively, which increased with the azobenzene contain for the copolymers.

Keywords: Azobenzene; Reversible addition-fragmentation chain transfer (RAFT) polymerization; tetrazole; photoisomerization behavior

1. Introduction

In recent years, polymeric materials containing azobenzene chromophore have drawn widespread attention due to their unique optical *trans-cis-trans* isomerization [1-4], which can be potentially applied in many fields, such as optical data storage [5,6], liquid crystal display [7-9], photoinduced birefringence [10], and holographic surface relief grating [11,12]. As well known, the photoresponsive behavior of azobenzene polymers is based on reversible *trans-cis-trans* photoisomerization of the azobenzene chromophore and possibly large-scale mass movement of the rigid azobenzene chromophore [11-15]. The *trans-cis* isomerization behavior of azobenzene was adjusted by the substituting groups [16]. With different substituting groups on azobenzene ring, azobenzene chromophore can be separated into three spectroscopic classes: azobenzene type, aminoazobenzene type and pseudo-stilbene type [17]. Among them, pseudo-stilbene azobenzene, which was substituted at the 4 and 4' positions with an electron-donor and an electron-acceptor groups, can be useful in optical isomerization applications due to the strong asymmetric electron distribution. The heterocyclic azobenzene groups were widely used as electron-acceptor because of their special push-pull chromophores as corresponding aryl analogues [18]. Based on this, azobenzene polymers containing heterocyclic groups are of great interest for their good film forming ability and potential applications in second-order molecular NLO properties [19], photo-responsive amphiphilic materials [20], photo-induced birefringence [21] and so on.

In this paper, a special heterocyclic substituting group, tetrazole, was introduced into the 4-position of azobenzene. The tetrazole compound showed characteristic property for their considerable energy and nitrogen content. It showed many significant applications in the fields of biomedical, ecological and agricultural sciences [21,22]. "Living"/controlled free radical polymerizations (LFRP) were used to synthesize polymers with predetermined structure. This unique technique offered a powerful tool to design azobenzene polymers with well-defined architectures, such as homopolymers [23,24], block copolymers [25-27], star polymers [28-30], graft copolymers [31] and so on. The typical LFRP systems included atom transfer radical polymerization (ATRP) [32-35], reversible addition-fragmentation chain transfer (RAFT) polymerization [36-39], nitroxide-mediated radical polymerization (NMP) [40-42], and so on. Many references reported successfully synthesizing well-defined azobenzene homopolymers and copolymers by LFRP technology [24-29]. As the alternative selection, RAFT polymerization was a much better technique to synthesize well defined polymers containing heterocyclic group for its wide range monomer suitability [21,23].

Following these basis, we reported the synthesis and characterization of novel methacrylate monomer with the tetrazole and azobenzene groups, 4′-(2-metharyloxyethyl)methylamino-4-(5-chlorotetrazol-1-yl)azobenzene (MACA), and incorporated into polymeric backbones by the RAFT technique. The homopolymer (PMACA) and diblock copolymers (PMMA-*b*-PMACA) were obtained with well-defined molecular weights and relatively narrow molecular weight distributions. Photo-responsive surface relief gratings (SRGs) behaviors of these polymers were investigated. Particularly, electrochemical behavior of azobenzene polymers with their *cis* and *trans* form was investigated by cyclic voltammetry (CV).

2. Experimental section

2.1. Materials

Methyl methacrylate (MMA; analytical grade; Shanghai Chemical Reagent Co. Ltd, Shanghai, China) was washed with an aqueous solution of sodium hydroxide (5 wt %) three times and then washed with deionized water until neutralization. After being dried with anhydrous magnesium sulfate, the monomer was distilled twice under reduced pressure, and kept below 0 ^{o}C. Azobisisobutyronitrile (AIBN; 99%, Shanghai Chemical Reagent Co. Ltd, Shanghai, China) was recrystallized three times from ethanol and dried in vacuum at room temperature overnight. Dimethyl formamide (DMF; analytical reagent; Shanghai Chemical Reagent Co. Ltd, Shanghai, China) was purified by vacuum distillation over anhydrous calcium hydroxide (CaH_2). Chloroform (analytical reagent), tetrahydrofuran (THF; analytical reagent) and triethylamine (TEA; analytical reagent) were purchased from Shanghai Chemical Reagent Co. Ltd. (Shanghai, China) and used after distillation. 5-Chloro-1-phenyl-1*H*-tetrazole (98%; Aldrich) and *N*-(2-hydroxyethyl)-*N*-methylaniline (Tokyo Kasei Kogyo Co., Ltd, Japan) were used as received. Other reagents were used without further purification. 2-Cyanoprop-2-yl dithiobenzoate (CPDB; >98%) was synthesized according to the method described in the literature [43].

2.2. Synthesis of 4′-(2-metharyloxyethyl)methylamino-4-(5-chloro-tetrazol-1-yl)azobenzene (MACA)

The novel methacrylate monomer (MACA) containing azobenzene chromophore and tetrazole moiety was synthesized following the synthetic pathway as shown in scheme 1.

(*Scheme 1. is here*)

2.2.1. 5-Chloro-1-(4-nitrophenyl)tetrazole (1)

The compound 1 was synthesized according to the literature [44]: 5-chloro-1-phenyl-1*H*-tetrazole (10.0 g, 56.0 mmol) was added slowly to fuming nitric acid (30 mL) in a 100 mL flask under vigorous stirring. The reaction was heated at 100 ^{o}C for 5 min. Subsequently, the hot mixture was poured onto a large excess of ice. The thick yellow precipitate was filtered off, washed with water several times, and dried in vacuum at room temperature. Recrystallization from ethanol gave the target product 1 (10.0 g, 79.2%) as yellow plates. The characteristic analytical data involved are as follows: ^{1}H NMR (400 MHz, $CDCl_3$, ppm): 8.46-8.56(d, 2H, ArH), 7.86-8.02 (d, 2H, ArH). ^{13}C NMR (100 MHz, $CDCl_3$, ppm): 148.75, 137.13, 125.46 and 125.17 (aromatic carbons), 145.47 (tetrazole carbon). IR (KBr, cm^{-1}): 3116, 3087, 3066, 2871, 1928, 1612, 1598, 1529, 1500, 1443, 1429, 1417, 1400, 1379, 1356, 1322, 1306, 1267, 1251, 1117, 1103, 1072, 1031, 1012, 982, 962, 858, 751, 728, 712, 688. 577, 516, 488, 442. Anal. calcd for $C_7H_4ClN_5O_2$: C 37.27, H 1.79, N 31.04; found: C 37.03, H 1.74, N 31.05. m. p.: 98.1 ^{o}C.

2.2.3. 1-(4-Aminophenyl)-5-chlorotetrazole (2)

Compound 2 was synthesized according to the following procedure [45]: a mixture of iron powder (2.30 g, 60.0 mmol) and ammonium chloride solution (5.30 g, 100 mmol) in 50 mL of distilled water was first prepared in a 500 mL flask under vigorous stirring. Then a 200 mL methanolic solution of compound 1 (4.50 g, 20.0 mmol) was added dropwise into this mixture over 10 min at room temperature. The resultant mixture was stirred under gentle reflux for 5 h. The inorganic residue was filtered and the methanol was evaporated under vacuum. The desired product precipitating out from the solution was collected by filtration, washed with water, dried under vacuum, and then recrystallized three times from methanol. The pure product 2 (3.00 g, yield: 76.9%) was obtained as pale plates. The characteristic data involved are as follows: ^{1}H NMR (400 MHz, DMSO-d_6, ppm): 7.26-7.30 (d, 2H, ArH), 6.66-6.72 (d, 2H, ArH), 5.79 (s, 2H, ArH). ^{13}C NMR (100 MHz, $CDCl_3$, ppm): 148.83, 122.74, 114.99 and 125.17 (aromatic carbons), 145.76 (tetrazole carbon). IR (KBr, cm^{-1}): 3416, 3321, 3212, 2965, 2931, 2855, 1887, 1642, 1604, 1511, 1455, 1422, 1407, 1312, 1289, 1258, 1245, 1180, 1143, 1112, 1088, 1040, 1006, 981, 832, 722. Anal. calcd for $C_7H_6ClN_5$: C 42.98, H 3.09, N 35.8; found: C 42.47, H 3.04, N 35.16. m. p.: 143.1 ^{o}C.

2.2.4. 4′-(2-Hydroxyethyl)methylamino-4-(5-chloro-tetrazol-1-yl)azobenzene (3)

Compound 2 (1.95 g, 10.0 mmol) was dissolved in concentrated HCl (4 mL) and deionized water (16 mL) at 70 ^{o}C. The mixture was stirred at 0-5 ^{o}C in an ice bath, and then aqueous solution (2 mL) of sodium nitrite (0.70 g) was added slowly. The mixture was stirred at 0-5 ^{o}C for 30 min. A solution of *N*-(2-hydroxyethyl)-*N*-methylaniline (1.50 g, 10.0 mmol) in acetic acid (5 mL) and deionized water (5 mL) was cooled to 0 ^{o}C and added into the above mixture under vigorous stirring at 0-5 ^{o}C. The pH of final mixture was adjusted to pH 5-6 using a NaOH (40%) solution. It was stirred for further 3 h at 0-5 ^{o}C. Then the reaction solution was added to a large amount of NaOH solution (40%) under stirring, and a red-orange precipitate formed. The desired precipitate was collected by filtration, washed with deionized water several times, and dried under vacuum. The crude products were recrystallized three times from ethanol to afford pure azobenzene-containing product 3 as red-orange crystal (3.00 g, yield: 83.8%). The characteristic data involved are as follows: ^{1}H NMR (400 MHz, $CDCl_3$, ppm): 7.98-8.07 (d, 2H, ArH), 7.80-7.96 (d, 2H, ArH), 7.57-7.73 (d, 2H, ArH), 6.73-6.90 (d, 2H, ArH), 3.83-3.96 (m, 2H, -CH_2-O), 5.59-3.70 (m, 2H, N-CH_2-), 3.18 (s, 3H, N-CH_3), 1.67 (s, 1H, OH). ^{13}C NMR (100 MHz, $CDCl_3$, ppm): 154.24, 152.55, 143.75, 132.27, 125.77, 125.07, 123.44, and 111.72 (aromatic carbons), 145.55 (tetrazole carbon), 60.33 (-N*C*$H_2$$CH_2$-OH)). 54.62 (-NCH$_2$*C*H$_2$-OH), 39.33 (-N*C*H$_3$). IR (KBr, cm^{-1}): 3443, 2951, 2931, 2855, 1599, 1558, 1516, 1501, 1500, 1428, 1416, 1396, 1372, 1328, 1308, 1277, 1246, 1192, 1139, 1104, 1085, 1039, 1029, 1004, 957, 845, 830. Anal. calcd for $C_{16}H_{16}ClN_7O$: C 53.71, H 4.51, N 27.40; found: C 53.31, H 4.34, N 27.51. m. p.: 145.9 ^{o}C.

2.2.5. 4′-(2-Metharyloxyethyl)methylamino-4-(5-chlorotetrazol-1-yl)azobenzene (MACA)

Compound 3 (1.78 g, 5.0 mmol), freshly distilled THF (50 mL), and freshly distilled triethylamine (1.07 g, 10.5 mmol) was added to a 250 mL three-necked flask. The solution was stirred in an ice bath. Methacryloyl chloride (0.960 mL, 10.0 mmol) diluted in dry THF (10 mL) was added to the cool stirred mixture dropwise. The reaction mixture was vigorously stirred for 3 h at 0-5 ^{o}C and then at room temperature overnight. The mixture was filtered, and the filtrate was evaporated under vacuum. The remaining yellow mixture was dissolved in dichloromethane and washed with 5% Na_2CO_3 aqueous solution and deionized water three times, then dried with anhydrous $MgSO_4$ overnight. The final crude product was purified by column chromatography (silica gel, EtOAc / petroleum ether = 1:3) to yield saffron solid (1.32 g, 62.1%). The characteristic analytical data involved are as follows: ^{1}H NMR (400 MHz, $CDCl_3$, ppm): 8.02-8.11(d, 2H, ArH), 7.88-7.98 (d, 2H, ArH), 7.67-7.76 (d, 2H, ArH),

6.81-6.90 (d, 2H, ArH), 6.08 (s, 1H, =CH), 5.58 (s, 1H, =CH), 4.30-4.48 (m, 2H, -CH_2-O), 3.73-3.87 (m, 2H, N-CH_2-), 3.16 (s, 3H, N-CH_3), 1.92 (s, 3H, C-CH_3). ^{13}C NMR (100 MHz, $CDCl_3$, ppm): 167.27 (O*C*=O), 154.19, 152.00, 143.75, 132.27, 125.75, 125.06, 123.44, and 111.58 (aromatic carbons), 145.52 (tetrazole carbon), 135.96 (-*C*H(CH_3)=CH_2), 126.23 (-CH(CH_3)=*C*H_2), 61.71 (-NCH_2*C*H_2O-), 50.84 (-N*C*H_2CH_2O-). 39.03 (-N*C*H_3), 18.34 (-CH(*C*H_3)=CH_2). IR (KBr, cm^{-1}): 2955, 2922, 2854, 1706, 1602, 1557, 1519, 1501, 1450, 1421, 1397, 1378, 1335, 1315, 1294, 1245, 1212, 1170, 1150, 1138, 1106, 1068, 1031, 1018, 1004, 976, 950, 849, 822, 748, 710, 698. Anal. calcd for $C_{20}H_{20}ClN_7O_2$: C 56.41, H 4.73, N 23.02; found: C 56.27, H 4.58, N 23.38. m. p.: 127.6 ^{o}C.

The ^{1}H NMR spectrum of MACA is shown in Figure 1.

(*Figure 1. is here*)

2.3. Preparation of the homopolymers (PMACA1, PMACA2, PMACA3) by RAFT polymerization

The general procedure was as following: MACA (0.425 g, 1.0 mmol), AIBN (1.10 mg, 0.0067 mmol), CPDB (4.40 mg, 0.02 mmol) was dissolved in freshly distilled DMF (2 mL) and added to a dry 5 mL ampule tube. The contents were purged with argon for 15 min to eliminate the oxygen. The ampule was flame-sealed and dropped into a preheated oil bath maintained at 70 ^{o}C. After 6 h polymerization, the ampule was opened, and the contents were diluted with THF (5 mL) and precipitated into methanol (250 mL). The precipitation process was carried out three times. The polymer (PMACA1) was dried to a constant weight at room temperature in vacuum. The conversion of PMACA1 was determined by gravimetry. Other polymers (PMACA2, PMACA3) were prepared in the same way with different polymerization time. The characteristic analytical data involved are as follows: ^{1}H NMR (400 MHz, $CDCl_3$, δ): 8.3-7.4 (ArH), 7.2-6.4 (ArH), 4.4-3.7 (COOCH_2C-), 3.7-3.4 (ArNCH_2C-), 3.1-2.6 (ArNCH_3), 2.0-1.3 (-CH_2-), 1.3-0.2 (-CCH_3). IR (KBr, cm^{-1}): 2951, 2844, 1706, 1602, 1518, 1435, 1380, 1245, 1004, 847, 748.

2.4. Preparation of the macro-RAFT agent (PMMA)

The macro-RAFT agent (PMMA) was prepared as following: a dry 2 mL ampule tube with a stir bar was filled with MMA (1.0 mL, 9.46 mmol), CPDB (25.1 mg, 0.114 mmol), AIBN (3.10 mg, 0.019 mmol) and freshly distilled DMF (0.5 mL). After purged with argon for 15 min, the ampule was flame-sealed. The polymerization was performed in an oil bath at 60 ^{o}C

for 12 h. Afterwards, the seal of ampule was opened, and the contents were diluted with THF (5 mL) and precipitated into methanol (250 mL). The polymer (PMMA) was obtained by filtration and dried to a constant weight at room temperature in vacuum. The conversion was 83.1% (0.7858 g) determined by gravimetry. The polymer molecular weight determined by GPC ($M_{n\,(GPC)}$) was 8300 g/mol (M_w/M_n = 1.14). The characteristic analytical data involved are as follows: ^{1}H NMR (400 MHz, $CDCl_3$, ppm): 8.1-7.9 (ArH), 7.5-7.3 (ArH), 3.9-3.4 (-OCH_3), 2.2-1.3 (-CH_2-), 1.3-0.4 (-CCH_3). ^{13}C NMR (100 MHz, $CDCl_3$, ppm): 179.5-176.0 (O*C*=O), 55.0-52.3 (-*C*H_2-C), 52.1-51.5 (O*C*H_3), 45.6-44.2 (-*C*(CH_3)CH_2), 19.4-15.8 (C-*C*H_3). IR (KBr, cm^{-1}): 2994, 2951, 1730, 1487, 1448, 1387, 1273, 1246, 1194, 1148, 1063, 987, 912, 841, 750.

2.5. Preparation of the block copolymers (PMMA-*b*-PMACAs)

The synthetic routes of the block copolymers (PMMA-*b*-PMACAs) were shown in Scheme 2. PMMA-*b*-PMACAs were synthesized with similar procedures for PMACA except that PMMA was used as macro-RAFT agent instead of CPDN. MACA (0.425 g, 1.0 mmol), AIBN (0.550 mg, 0.0033 mmol), PMMA (0.166 g, 0.02 mmol) and freshly distilled DMF (3 mL) were charged in a dry 5 mL ampule tube with a stir bar, and then stirred for 10 min until a homogeneous solution was formed. After purged with argon for 15 min, the ampule was flame-sealed, and put in an oil-bath at 70 ^{o}C for 24 h. The reactant was diluted by THF (5 mL), precipitated into methanol (250 mL), and the purification process was carried out three times. The final product (PMMA-*b*-PMACA3) was dried to a constant weight at room temperature in vacuum. Other block copolymers were prepared using similar procedures. The characteristic analytical data involved are as follows: ^{1}H NMR (400 MHz, $CDCl_3$, ppm): 8.3-7.5 (ArH), 7.0-6.4 (ArH), 4.3-3.6 ($COOCH_2$C-), 3.6-3.4 ($ArNCH_2$C- and -OCH_3), 3.1-2.6 ($ArNCH_3$), 2.1-1.3 (-CH_2-), 1.3-0.2 (-CCH_3). ^{13}C NMR (100 MHz, $CDCl_3$, ppm): 178.6-176.5 (O*C*=O), 167.35-167.15, 155.0-150.5, 144.0-142.5, 133.0-131.0, 127.0-121.0, 112.5-111.0 (aromatic carbons), 146.0-144.5 (tetrazole carbon), 61.8-61.6 (-NCH_2*C*H_2O-), 54.9-52.2 (-N*C*H_2CH_2O- and -*C*H_2-C), 52.1-51.5 (O*C*H_3), 45.7-44.1 (-*C*(CH_3)CH_2), 39.5-38.0 ($ArNCH_3$), 19.4-15.8 (C-*C*H_3). IR (KBr, cm^{-1}): 2993, 2951, 2840, 1730, 1602, 1518, 1435, 1381, 1246, 1146, 991, 845, 750.

(*Scheme 2. is here*)

2.6. Preparation of the PMMA-*b*-PMACA film and optical characterization.

A $CHCl_3$ solution of the PMMA-*b*-PMACA1 (0.05 g/mL) was filtered through 0.2 μm pore size filter, and the thin film was obtained via spin-coating the solution onto clean glass slide at 3500 rpm. The thickness of homogeneous thin films was measured to be about 332 nm by Ambios Technology XP-2 Stylus Profiler and subsequently dried under vacuum for 24 h at room temperature. The other polymers films were also obtained using the same method , and the thicknesses were 312 nm (PMMA-*b*-PMACA2) and 350 nm (PMMA-*b*-PMACA3), respectively. The films were allowed to store in a desiccator for further study. The procedure for SRGs fabrication could be found in a related reference [4].

2.6. Characterizations

^{1}H NMR spectra of the polymers were recorded on an INOVA 400 MHz nuclear magnetic resonance instrument, using $CDCl_3$ or DMSO-d_6 as the solvent and tetramethylsilane (TMS) as the internal standard. ^{13}C NMR spectra were run on the same instrument operating at 100 MHz at room temperature and the chemical shifts were recorded under similar conditions. The molecular weights (M_ns) and molecular weight distributions (M_w/M_ns) of the polymers were determined with a Waters 1515 gel permeation chromatographer (GPC) equipped with refractive index detector, using HR1, HR3, and HR4 column with molecular weight range 100-500,000 calibrated with PS or PMMA standard samples. THF was used as the eluent at a flow rate of 1.0 mL min^{-1} operated at 30 ^{o}C. Elemental analysis of C, H and N were measured with an EA1110 CHNO-S instrument. The UV absorption spectra of the samples in chloroform solution were determined on a shimadzu-RF540 spectrophotometer at room temperature. Thermal analysis of the polymers and melting points (m. p.) of all the compounds were performed by differential scanning calorimetry (DSC) using a TA instruments DSC2010 with a heating/cooling rate of 10 ^{o}C min^{-1} under a continuous nitrogen flow. FT-IR spectra were recorded on a Perkin-Elmer 2000 FT-IR spectrometer. Thermogravimetric analysis (TGA) was performed at a heating rate of 20 ^{o} C/min from room temperature to 750 ^{o} C under a continuous nitrogen flow of 50 mL min^{-1} with a TA Instruments SDT-2960TG/DTA. Cyclic voltammograms were performed on a CHI631B electrochemical workstation at a constant scan of 0.1 V/s. Measurements were carried out in a conventional three-electrode cell. The working electrode was an argentum electrode and counter electrode was an argentum mesh. The 0.1 mmol polymers were dissolved in 10 mL chloroform containing 0.1 M tetra-*n*-butylammonium hexafluorophosphate ((*n*-Bu)$_4$NPF$_6$) as the supporting electrolyte.

3. Results and discussion

3.1. Polymer synthesis

RAFT polymerization of the synthesized monomer (MACA) was carried out using CPDB as RAFT agent and AIBN as initiator in DMF at 70 ^{o}C, and homopolymers (PMACA1, PMACA2 and PMACA3) were obtained under different reaction time with a molar ratio of $[MACA]_0 : [CPDB]_0 : [AIBN]_0 = 300 : 3 : 0.5$. As showed in Table 1, after 3 h, 6 h and 12 h polymerization, PMACA1, PMACA2 and PMACA3 were obtained with the monomer conversions of 15.2 %, 23.5 % and 62.7 %, respectively. The molecular weight distributions (M_w/M_ns) measured by GPC were relatively narrow ($M_w/M_n \leq 1.30$) and the number-average molecular weights measured by GPC ($M_{n\ (GPC)}$) increased with monomer conversions, which indicated that the polymerization was conducted under a controlled manner. However, there were slightly discrepancies between the molecular weights ($M_{n\ (GPC)}$s) obtained by GPC and the theoretical values ($M_{n\ (th)}$s), which may be due to the incomplete usage of RAFT agent (CPDB) and the poly(methyl methacrylate) (PMMA) standards used for GPC calibration [46,47].

(*Table 1. is here*)

The film forming property is very important for the photo-responsive materials of azobenzene polymers [11]. We find that PMACA showed poor film forming abilities. Thus, the block copolymers containing MACA and MMA as structural units were designed to improve forming properties of azobenzene polymers. However, the attempt for preparing block copolymer using PMACA as macro-RAFT agent for MMA polymerization was failed, and the obtained block copolymers have broader molecular weight distributions ($M_w/M_n >$ 1.50) with still several homopolymer (PMACA) chains, possibly due to the presence of "dead" polymer chains in the original polymer [12]. Thus, the alternative way was used here, e.g. by using PMMA as the macro-RAFT agent to conduct RAFT polymerization of MACA. PMMA was firstly prepared by RAFT polymerization of MMA using CPDB as RAFT agent. The $M_{n\ (GPC)}$ and M_w/M_n of PMMA was 8300 g/mol and 1.14 (determined by GPC), respectively, which was showed in the Table 1. Diblock copolymers (PMMA-*b*-PMACAs) with different azo-containing compositions were obtained by adjusting the polymerization time ($[MACA]_0 : [PMMA]_0 : [AIBN]_0 = 300 : 3 : 0.5$, AIBN as initiator in DMF at 70 ^{o}C). The results of block copolymers were summarized in Table 1, and these block copolymers were prepared with predetermined molecular weights and narrow molecular weight

distributions. Most of all, the obtained block copolymers showed good solubility in $CHCl_3$, and good film forming ability. The GPC curves of the polymers in Figure 2 indicated that almost the entire macro-RAFT agent (PMMA) was transferred into block copolymers. It suggested that the macro-RAFT agent (PMMA) was an efficient RAFT agent for the chain-extension polymerization of MACA.

(*Figure 2. is here*)

3.2. Structural characterization of polymers

To confirm the molecular structures, polymers were characterized by FT-IR, ^{1}H NMR and ^{13}C NMR spectra. The FT-IR spectra of these polymers were given in Figure 3. For comparison, the spectra of MACA, PMMA ($M_{n\ (GPC)}$ = 8300 g/mol, M_w/M_n = 1.14), and the block polymer (PMMA-*b*-PMACA3, $M_{n\ (GPC)}$ = 10200 g/mol, M_w/M_n = 1.28) were shown in the same figure. The FT-IR spectrum of the monomer, MACA, showed the characteristic signal at 1706 and 1602 cm^{-1} due to the stretching vibrations of carbonyl and azobenzene group. The FT-IR spectrum of PMMA showed the characteristic carbonyl peek at 1730 cm^{-1} [48-52]. After chain-extension, PMMA-*b*-PMACA3 showed strong absorption of the stretching vibration of carbonyl group and azobenzene group at 1730 and 1602 cm^{-1}, respectively. The peak at 1706 cm^{-1} corresponding to carbonyl group of MACA was merged with the 1730 cm^{-1} peak in the FT-IR spectrum of copolymer. The FT-IR spectra confirmed the structure of block copolymer.

(*Figure 3. is here*)

Figure 4 showed the ^{1}H NMR spectroscopy of PMMA, PMACA3, and PMMA-*b*-PMACA3, respectively. In spectrum of PMMA, the chemical shifts at the range from 3.4 to 3.9 ppm and 0.4 to 2.2 ppm were due to protons in the PMMA chains [53]. The weak signals at the range from 7.3 to 8.1 ppm were attributed to the aromatic protons in CPDB structure, which confirmed that the RAFT agent was attached on the end of the PMMA chain. In the ^{1}H NMR spectroscopy of PMACA3, the characteristic signals corresponding to the aromatic protons of azobenzene group were observed at the range of 6.4-7.0 ppm and 7.5-8.3 ppm. The signals from 0.2 to 4.4 ppm were assigned to the methenyl and methyl protons in the polymer chain. However, the resonances of characteristic signals of the aromatic protons at CPDB

moieties were overlapped by the phenyl groups of polymer, and thus these cannot be discernable in this spectroscopy.

In the ^{1}H NMR spectroscopy of PMMA-*b*-PMACA3 (Figure 4, PMMA-*b*-PMACA3), the characteristic signals corresponding to all protons in PMMA-*b*-PMACA3 were in accordance with theoretical chemical shifts. For example, the chemical shifts at 6.4-7.0 ppm ("a" in Figure 4 (PMMA-*b*-PMACA3)) and 7.5-8.3 ppm ("b" in Figure 4 (PMMA-*b*-PMACA3)) were ascribed to the aromatic protons of azobenzene group, and the signals of methyl protons ("d" in Figure 4 (PMMA-*b*-PMACA3)) in the PMMA were observed from 3.4 ppm to 3.6 ppm. Furthermore, the molecular weight of the block copolymer ($M_{n\ (NMR)}$) could be calculated from the ratio of the characteristic signals in the ^{1}H NMR spectroscopy from equation (1).

$$M_{n(NMR)} = M_{PMMA} + \left(\frac{I_{7.5\text{-}8.0}}{6} / \frac{I_{3.4\text{-}3.6}}{3}\right) \times \frac{M_{PMMA}}{M_{MMA}} \times M_{MACA} \quad (1)$$

where $I_{7.5\text{-}8.0}$ is the integral of the signals at 7.5-8.0 ppm ("a" in Figure 4 (PMMA-*b*-PMACA3)), and $I_{3.4\text{-}3.6}$ is the integral of the signals at 3.4-3.6 ppm ("d" in Figure 4 (PMMA-*b*-PMACA3)).

The calculated molecular weights ($M_{n\ (NMR)}$) listed in Table 1 were close to those theoretical value, which further confirmed the well-defined structure of the obtained block copolymers.

(*Figure 4. is here*)

To further demonstrate the polymer structures, the ^{13}C NMR spectroscopy of PMMA and PMMA-*b*-PMACA3 were shown in Figure 5. The chemical shifts of the carbonyl carbons (-O*C*=O) adjacent to the MMA main chain could be found between 179.5 and 176.0 ppm ("a") in ^{13}C NMR spectrum of PMMA, and the visible shifts from 52.1 to 51.5 ppm ("b") corresponded to the methyl carbons (O*C*H$_3$). In the aliphatic carbons region, three broad peaks (55.0-52.3 ppm, 45.6-44.2 ppm and 19.4-15.8 ppm) were also related to the MMA main chain, which were in good agreement with PMMA. In the ^{13}C NMR spectroscopy of PMMA-*b*-PMACA3 (Figure 5 PMMA-*b*-PMACA3), the characteristic signals corresponding to all carbons in PMMA-*b*-PMACA3 were in accordance with the polymer chemical shifts. The aromatic carbons in azobenzene group were observed in chemical shifts including 167.35-167.15 ppm, 155.0-150.5 ppm, 144.0-142.5 ppm, 133.0-131.0 ppm, 127.0-121.0 ppm and

112.5-111.0 ppm. The most important were the tetrazole carbon ("c") signals at the range from 146.0 to 144.5 ppm, which could not be confirmed through in the ^{1}H NMR spectroscopy.

(*Figure 5. is here*)

3.3. Thermal properties of the polymers

Thermal properties of the polymers were evaluated by differential scanning calorimetry (DSC). The second DSC heating curves of PMMA and copolymers (PMMA-*b*-PMACA1, PMMA-*b*-PMACA2 and PMMA-*b*-PMACA3) were given in Figure 6. The DSC characterizations were carried out with a heating/cooling rate of 10 ^{o}C min^{-1} under a continuous nitrogen flow. From Figure 6, all of the polymers showed glass transition temperature (T_g). The T_g of PMMA was about 123 ^{o}C, and the T_g of PMMA-*b*-PMACA1, PMMA-*b*-PMACA2 and PMMA-*b*-PMACA3 were 133 ^{o}C, 134 ^{o}C and 141 ^{o}C, respectively. PMACA3 had a much higher T_g (140 ^{o}C) than PMMA (123 ^{o}C), which meant that introduction of rigid azobenzene chromophore into PMMA chain obviously improved the T_g of the polymers. As shown in Figure 5, there was only one glass transition point observed in all the block copolymers, and the polymers with higher PMACA content showed higher values of T_g. That indicated that PMMA and PMACA segments displayed the phase mixing at the broad molecular region. The glass transition temperature of PMMA-*b*-PMACA3 (141 ^{o}C) is a little higher than PMACA3, because the molecular weight of PMACA in block copolymer (11300 g/mol) is a little higher than that of PMACA3 (10200 g/mol). Moreover, there was no melting point observed in these DSC curves of polymers, which indicated that all the polymers were amorphous. Figure 6 showed the wide-angle X-ray diffraction (WAXD) results of PMMA and PMMA-*b*-PMACA. There is no sharp peak observed, which indicated that these polymers were amorphous.

Thermal properties of the polymers were also evaluated by the thermogravimetric analysis (TGA) under a continuous nitrogen flow [54], and the results were shown in Figure 8. PMMA was thermally stable up to 216 ^{o}C with about 5% weight loss, and lost 10% of its weight at the temperature of 252 ^{o}C, which could be attributed to the missing of the methyl carbons (OCH_3). Similarly, PMMA-*b*-PMACA3 has 5% weight degradation at the temperature of 196 ^{o}C, which was lower than that of PMMA, and the reason may be due to unstable ester structure and aliphatic segment (-$OCH_2CH_2N(CH_3)$). There was about 25% of weight loss at the first stage (215 ^{o}C). Due to introduction of azobenznene and tetrazole groups, the weight loss of

PMMA-*b*-PMACA3 slowed down, and about 26% of carbon remained at 750 ^{o}C. The remainder mass increased with the higher PMACA content in PMMA-*b*-PMACAs.

(*Figure 6. is here*)

(*Figure 7. is here*)

(*Figure 8. is here*)

3.4. Photoisomeriztion behavior

As well known, azobenzene polymers exhibit photoisomeriztion behavior, which undergoes isomerization from *trans*- to *cis*-forms under 365 nm UV irradiation [55]. Here, photoisomeriztion of PMMA-*b*-PMACA in chloroform solution was studied under irradiation with 365 nm UV light. The UV-vis absorption spectra were recorded at different time intervals until photo-stationary state was reached. The representative results for PMMA-*b*-PMACA3 ($M_{n\ (GPC)}$ = 19600 g/mol, M_w/M_n = 1.25) were given in Figure 9. As shown in Figure 9, PMMA-*b*-PMACA3 showed absorption at 430 nm before UV exposure, which was due to the characteristic intense of π-π^* transition (*trans*-form azobenzene). After irradiation with 365 nm UV light, the *trans*-form of the azobenzene changed to the *cis*-form, which showed characteristic absorption peak at 513 nm. It should be indicated that the absorption (430 nm) of *trans*-form azobenzene slightly increased upon UV irradiation in the beginning period of irradiation (3 minutes), which may be due to the bulky tetrazole substitution on the azobenzene. After UV irradiation of 3 minutes, the *trans*- form content of azobenzene reached a peak (Figure 9 A). With further increased irradiation time, the absorption of *trans*-form azobenzene at 430 nm decreased remarkable, and the intensity of the *cis*- form azobenzene (513 nm) increased rapidly. Furthermore, during the *tran*-*cis* isomerization, the absorption peak at 430 nm decreased too much, and embedded into the shoulder of and 513 nm peak spectra, which resulted in the appearance of a “red-shift” peak from 413 to 513 nm [56].

(*Figure 9. is here*)

The electrochemical behavior of polymers in solution before and after UV irradiation was investigated using the cyclic voltammetry (CV). The typical CV curves of PMMA-*b*-PMACA3 in chloroform solution before and after UV irradiation was showed in Figure 10. Before UV irradiation, the azobenzene stay in the *trans* form, and an oxidation peak at 1.0V was showed in the CV curve. After the 365 nm light irradiated for 80 min, almost all of the

azobenzene shifted to the *cis* form (from Figure 9), and the oxidation peak in CV curve obviously shifted to 0.6V. Thus, the electrochemical behavior can be adjusted by the UV irradiation, which may find their applications in photo electronic materials [57].

(*Figure 10. is here*)

3.5 Photoinduced surface relief gratings

The obtained PMMA-*b*-PMACAs with good film-forming property were investigated for the surface relief grating (SRG) ability. Thin films of PMMA-*b*-PMACAs via spin-coating on the clean glass were obtained, and the thicknesses were 332 nm (PMMA-*b*-PMACA1), 312 nm (PMMA-*b*-PMACA2) and 350 nm (PMMA-*b*-PMACA3), respectively. Then, the SRG measurement was performed with linearly polarized Kr^+ laser beam (413.1 nm, 200 mW/cm^2) at room temperature [4], and characterized by the inscription rates and the saturation levels of SRGs formation, which were detected using atomic force microscopy (AFM, NT-MDT SOLVER P47-PRO). Figure 11 showed AFM three-dimensional (A) and plane (B) images of the alternate surface relief structures with regular spaces fabricated on the PMMA-*b*-PMACA1 film surfaces after Kr^+ laser irradiation for 1600 s at room temperature. AFM images showed that the surface modulation depth was about 145.4 nm, and the grating spacing was about 1.45 μm, which was used as photoinduced data storage. When the polymer film was exposed to the writing beam for 1600 s, the rates of gratings formation were probed by measuring the first-order diffraction efficiency of the SRG. The increase of the diffraction efficiency of SRG with the irradiation time was shown in Figure 12. For the PMMA-*b*-PMACA1 sample, the diffraction efficiency rapidly increased to about 1.22% until saturation level at 1600 s. Moreover, the diffraction efficiency of SRG was affected by the azobenzene contain for the PMMA-*b*-PMACAs. From the Figure 12, the diffraction efficiency of the SRGs was 1.22 (PMMA-*b*-PMACA1), 2.38 (PMMA-*b*-PMACA2) and 3.02 (PMMA-*b*-PMACA3), respectively, which increased with the azobenzene contain of the copolymers.

(*Figure 11. is here*)

(*Figure 12. is here*)

4. Conclusion

A novel methacrylate monomer (4'-(2-methacryloxyethyl)methylamino-4-(5-chlorotetrazol-1-yl)azobenzene, MACA) containing azobenzene chromophore and tetrazole

moiety was successfully synthesized and polymerized to form homopolymers PMACAs and block copolymers (PMMA-*b*-PMACAs) via RAFT technology. These obtained polymers with controlled molecular weights and narrow molecular weight distributions (M_w/M_ns <1.30) were confirmed by ^{1}H NMR spectroscopy and gel permeation chromatography (GPC). These copolymers showed moderate *trans-cis* isomerization behavior, as most of the azobenzene polymers. Cyclic voltammetry results of copolymer showed that the oxidation peak of copolymer shifted from 1.0V to 0.6V when azobenzene isomerization from *trans* to *cis* form. On irradiation with a linearly polarized Kr^+ laser beam (413.1 nm), The PMMA-*b*-PMACA1 film could formed the well-defined efficient surface relief grating (SRG) with the 145.4 nm surface modulation depth and 1.45 μm grating spacing. the diffraction efficiency of the SRGs were 1.22 (PMMA-*b*-PMACA1), 2.38 (PMMA-*b*-PMACA2) and 3.02 (PMMA-*b*-PMACA3), respectively, which increased with the azobenzene contain for the copolymers.

Acknowledgements: The financial supports of this work by the National Natural Science Foundation of China (Nos. 21104006), A Project Funded by the Priority Academic Program Development of Jiangsu Higher Education Institutions (PAPD), the Program of Innovative Research Team of Changzhou University (ZMF1002118).

References

[1] G. Kumar, D. C. Neckers, Chem. Rev. 89 (1989) 1915.

[2] D. Brown, A. Natansohn, P. Rochon, Macromolecules 28 (1995) 6116.

[3] A. Natansohn, P. Rochon, Chem. Rev. 102 (2002) 4139.

[4] X. Q. Xue, J. Zhu, Z. B. Zhang, N. C. Zhou, Y. F. Tu, X. L. Zhu, Macromolecules 43 (2010) 2704.

[5] W. M. Gibons, P. J. Shannon, S. T. Sun, B. J. Swetlin, Nature 351 (1991) 49.

[6] T. G. Pedersen, P. M. Johansen, H. C. Pedersen, J. Opt. A: Pure Appl. Opt. 2 (2000) 272.

[7] D. Hore, A. Natansohn, P. Rochon, J. Phys. Chem. B 107 (2003) 2197.

[8] H. R. Hafiz, F. Nakanishi, Nanotechnology 14 (2003) 649.

[9] A. Bobrovsky1, V. Shibaev, A. Bubnov, V. Hamplová, M. Kašpar, D. Pociecha, M. Glogarová, Macromol. Chem. Phys. 4 (2011) 342.

[10] L. M. Sáiz, P. A. Oyanguren, M. J. Galante, React. Funct. Polym. 72 (2012) 478.

[11] P. Rochon, E. Batalla, A. Natansohn, Appl. Phys. Lett. 66 (1995) 136.

[12] X. Q. Xue, J. Zhu, Z. B. Zhang, N. C. Zhou, X. L. Zhu, React. Funct. Polym. 70 (2010) 456.

[13] Y. Wu, A. Natansohn, P. Rochon, Macromolecules 37 (2004) 6090.

[14] C. Barrett, P. Rochon, A. Natansohn, J. Chem. Phys. 109 (1998) 1505.

[15] M. S. Ho, C. Barrett, J. Paterson, M. Esteghamatian, A. Natansohn, P. Rochon, Macromolecules 29 (1996) 4613.

[16] I. Mita, K. Horie, K. Hirao, Macromolecules 22 (1989) 558.

[17] T. Naito, K. Horie, I. Mita, Polym. J. 23 (1991) 809.

[18] U. Caruso, R. Diana, A. Fort, B. Panunzi, A. Roviello, Macromol. Symp. 234 (2006) 87.

[19] A. Facchetti, A. Abbotto, L. Beverina, M. E. van der Boom, P. Dutta, G. Evmenenko, T. J. Marks, G. A. Pagani, Chem. Mater. 14 (2002) 4996.

[20] J. Wei, Z. Yan, L. Lin, J. S. Gu, Z. Feng, Y. L. Yu, React. Funct. Polym. 73 (2013) 1009.

[21] L. P. Yu, Z. B. Zhang, X. R. Chen, W. Zhang, J. H. Wu, Z. P. Cheng, J. Zhu. X. L. Zhu, J. Polym. Sci. Part A: Polym. Chem. 46 (2008) 682.

[22] N. V. Tsarevsky, K. V. Bernaerts, B. Dufour, F. E. DuPrez, K. Matyjaszewski, Macromolecules 37 (2004) 9308.

[23] Y. Y. Zhang, Z. P. Cheng, X. R. Chen, W. Zhang, J. H. Wu, J. Zhu, X. L. Zhu, Macromolecules 40 (2007) 4809.

[24] M. Jin, Q. X. Yang, R. Lu, T. H. Xu, Y. Y. Zhao, J. Polym. Sci. Part A: Polym. Chem. 42 (2004) 4237.

[25] P. Forcen, C. Oriol, R. Sanchez, S. Alcala, Hvilsted, K. Jankova, J. Loos, J. Polym. Sci. Part A: Polym. Chem. 45 (2007) 1899.

[26] X. Q. Xue, J. Zhu, Z. B. Zhang, Z. P. Cheng, Y. F. Tu, X. L. Zhu, Polymer 51 (2010) 3083.

[27] W. Deng, P. A. Albouy, E. Lacaze, P. Keller, X. G. Wang, M. M. Li, Macromolecules 41 (2008) 2459.

[28] X. Li, X. M. Lu, Q. H. Lu, D. Y. Yan, Macromolecules 40 (2007) 3306.

[29] X. D. Tang, L. C. Gao, N. F. Han, X. H. Fan, Q. F. Zhou, J. Polym. Sci. Part A: Polym. Chem. 45 (2007) 3342.

[30] K. Gharagozloo-Hubmann, O. Kulikovska, V. Börger, H. Menzel, J. Stumpe, Macromol. Chem. Phys. 21 (2009) 1809.

[31] X. D. Tang, L. C. Gao, X. H. Fan. Q. F. Zhou, J. Polym. Sci. Part A: Polym. Chem. 45 (2007) 1653.

[32] M. Kato, M. Kamigaito, M. Sawamoto, T. Higashimura, Macromolecules 28 (1995) 1721.

[33] J. S. Wang, K. Matyjaszewski, Macromolecules 28 (1995) 7901.

[34] K. Matyjaszewski, J. Xia, Chem. Rev. 101 (2001) 2921.

[35] X. Q. Xue, W. Zhang, Z. P. Cheng, J. Zhu, X. L. Zhu, J. Polym. Sci. Part A: Polym. Chem. 46 (2008) 5626.

[36] J. Chiefari, Y. K. Chong, F. Ercole, J. Krstina, J. Jeffery, T. P. T. Le, R. T. A. Mayadunne, G. F. Meijs, C. L. Moad, G. Moad, E. Rizzardo, S. H. Thang, Macromolecules 31 (1998) 5559.

[37] G. Moad, E. Rizzardo, S. H. Thang, polymer 49 (2008) 1079.

[38] A. B. Lowe, C. L. McCormick, Prog. Sci. 32 (2007) 283.

[39] U. Georgi, P. Reichenbach, U. Oertel, L. M. Eng, B. Voit, React. Funct. Polym. 72 (2012) 242.

[40] G. Moad, E. Rizzardo, D. H. Solomon, Macromolecules 15 (1982) 909.

[41] C. J. Hawker, A. W. Bosman, E. Harth, Chem. Rev. 101 (2001) 3661.

[42] M. K. Georges, P. R. N. Veregin, P. M. Kazmaier, G. K. Hamer, Macromolecules 26 (1993) 2987.

[43] Y. K. Chong, J. Kristina, T. P. T. Le, G. Moad, A. Psotma, E. Rizzarid, S. H. Thang, Macromolecules 36 (2003) 2256.

[44] R. A. W. Johnstone, P. J. Pricet, J. Chem. Soc. Perkin Trans. 1 1069 (1987).

[45] K. Ramadas, N. Srinivasan, Syn. Commun. 22 (1992) 3189.

[46] G. Moad, E. Rizzardo, S. H. Thang, Aust. J. Chem. 58 (2005) 379.

[47] J. Krstina, T. P. T. Le, G. Moad, A. Postma, E. Rizzardo, S. H. Thang, Macromolecules 36 (2003) 2256.

[48] A. V. Raghu, G. S. Gadaginamath, N. T. Mathew, S. B. Halligudi, T. M. Aminabhavi, Reac. Funct. Polym. 67 (2007) 503.

[49] A. V. Raghu, G. S. Gadaginamath, M. Priya, P. Seema, H. M. Jeong,T. M. Aminabhavi, J. Appl. Polym. Sci. 110 (2008) 2315.

[50] A. V. Raghu, H. M. Jeong, J. H. Kim, Y. R. Lee, Y. B. Cho, K. Sirsalmath, Macromol. Res. 16 (2008) 194.

[51] K. R. Reddy, A. V. Raghu, H. M. Jeong, Polym. Bull. 60 (2008) 609.

[52] A. V. Raghu, G. S. Gadaginamath, S. S. Jawalkar, S. B. Halligudi and T. M. Aminabhavi, J. Polym. Sci., Part A:Polym. Chem. 44 (2006) 6032.

[53] X. Q. Xue, F. Li, W. Y. Huang, H. J. Yang, B. B. Jiang, Y. L. Zheng, D. L. Zhang, J. B. Fang, L. Z. Kong, G. Q. Zhai, J. H. Chen, Macromol. Rapid Commun. 35 (2014) 330.

[54] W. Y. Huang, C. Liu, H. J. Yang, X. Q. Xue, B. B. Jiang, D. L. Zhang, L. Z. Kong, Y. Zhang, S. Komarneni, Polym. Chem. 5 (2014) 3326.

[55] Z. D. Xu, Y. Zhang, X. H. Fan, X. H. Wan, Q. F. Zhou, Chinese J Polym. Sci. 20 (2002), 99.

[56] H. Z. Cao, W. Zhang, J. Zhu, X. R. Chen, Z. P. Cheng, J. H. Wu, X. L. Zhu, Express Polym. Lett. 2 (2008) 589.

[57] G. Klopman, N. Doddapaneni, J. Phys. Chem. 78 (1974) 1825.

Figure captions

Scheme 1. The synthetic route of 4′-(2-metharyloxyethyl)methylamino-4-(5-chlorotetrazol-1-yl)azobenzene (MACA).

Scheme 2. The synthetic route of block copolymers (PMMA-*b*-PMACA).

Figure 1. ^{1}H NMR spectrum of 4′-(2-metharyloxyethyl)methylamino-4-(5-chlorotetrazol-1-yl)azobenzene (MACA) in $CDCl_3$.

Figure 2. The GPC curves of PMMA, PMMA-*b*-PMACA1, PMMA-*b*-PMACA2, and PMMA-*b*-PMACA3.

Figure 3. The FT-IR spectroscopy of MACA, PMMA ($M_{n\,(GPC)}$ = 8300 g/mol, M_w/M_n = 1.14) and PMMA-*b*-PMACA3 ($M_{n\,(GPC)}$ = 19600 g/mol, M_w/M_n = 1.25).

Figure 4. ^{1}H NMR spectroscopy of PMMA ($M_{n\,(GPC)}$ = 8300 g/mol, M_w/M_n = 1.14), PMACA3 ($M_{n\,(GPC)}$ = 10200 g/mol, M_w/M_n = 1.28), and PMMA-*b*-PMACA3 ($M_{n\,(GPC)}$ = 19600 g/mol, M_w/M_n = 1.25) in DMSO-d_6.

Figure 5. ^{13}C NMR spectroscopy of PMMA ($M_{n\,(GPC)}$ = 8300 g/mol, M_w/M_n = 1.14) and PMMA-*b*-PMACA3 ($M_{n\,(GPC)}$ = 19600 g/mol, M_w/M_n = 1.25) in $CDCl_3$.

Figure 6. Second DSC heating curves of PMMA, PMMA-*b*-PMACA1, PMMA-*b*-PMACA2, PMMA-*b*-PMACA3, PMACA3.

Figure 7. WAXD spectra of PMMA, PMMA-*b*-PMACA1 and PMMA-*b*-PMACA3 at room temperature.

Figure 8. Thermogravimetric analysis (TGA) of PMMA, PMMA-*b*-PMACA1 and PMMA-*b*-PMACA3.

Figure 9. The UV-vis absorption changes of PMMA-*b*-PMACA3 during the irradiation with 365 nm UV light in chloroform solution at room temperature. The concentration of repeating units is 2.50×10^{-6} M. A: initial 3 minutes; B: after 3 minutes.

Figure 10. Cyclic voltammogams of PMMA-*b*-PMACA3 before and after the irradiation with 365 nm UV light in chloroform solution. The concentration of repeating units is 2.50×10^{-6} M in room temperature containing 0.1 M tetra-n-butylammonium hexafluorophosphate ($(n\text{-}Bu)_4NPF_6$) as the supporting electrolyte.

Figure 11. AFM images of the SRG formed on PMMA-*b*-PMACA1 film: (A) plane view of the SRG and (B) three-dimensional view of the SRG.

Figure 12. Diffraction efficiency as a function of the irradiation time for the similar thickness thin film of three samples (PMMA-*b*-PMACA1, 330 nm; PMMA-*b*-PMACA2, 312 nm; PMMA-*b*-PMACA3, 350 nm).

Table 1. Characteristics of PMMA, PMACAs and PMMA-*b*-PMACAs

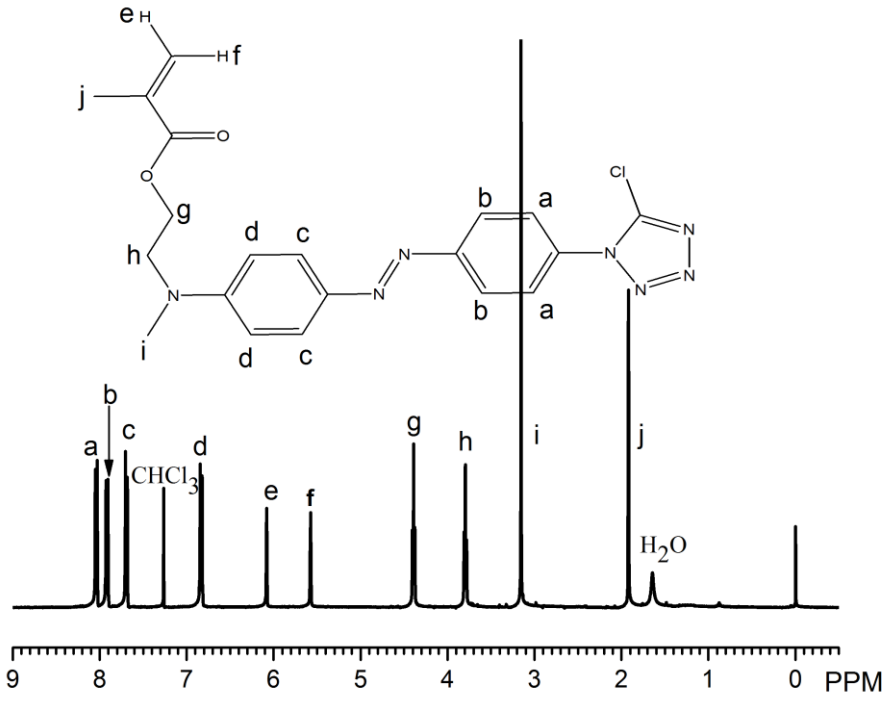

Figure 1

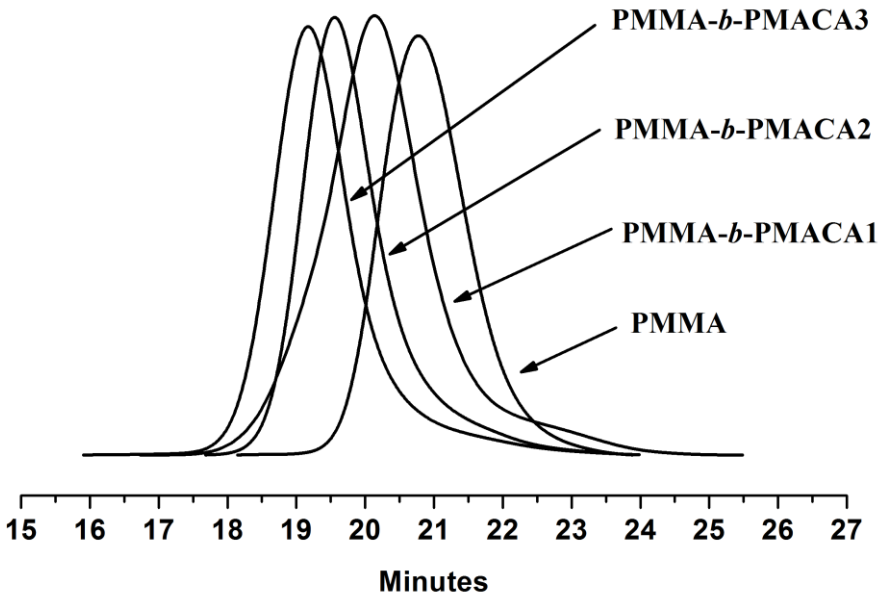

Figure 2

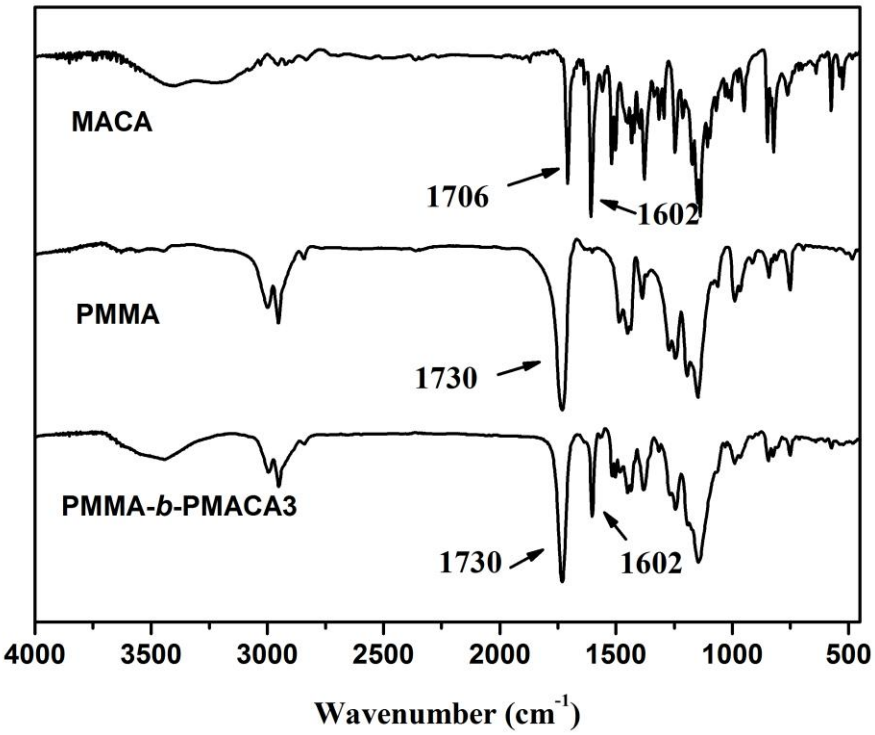

Figure 3

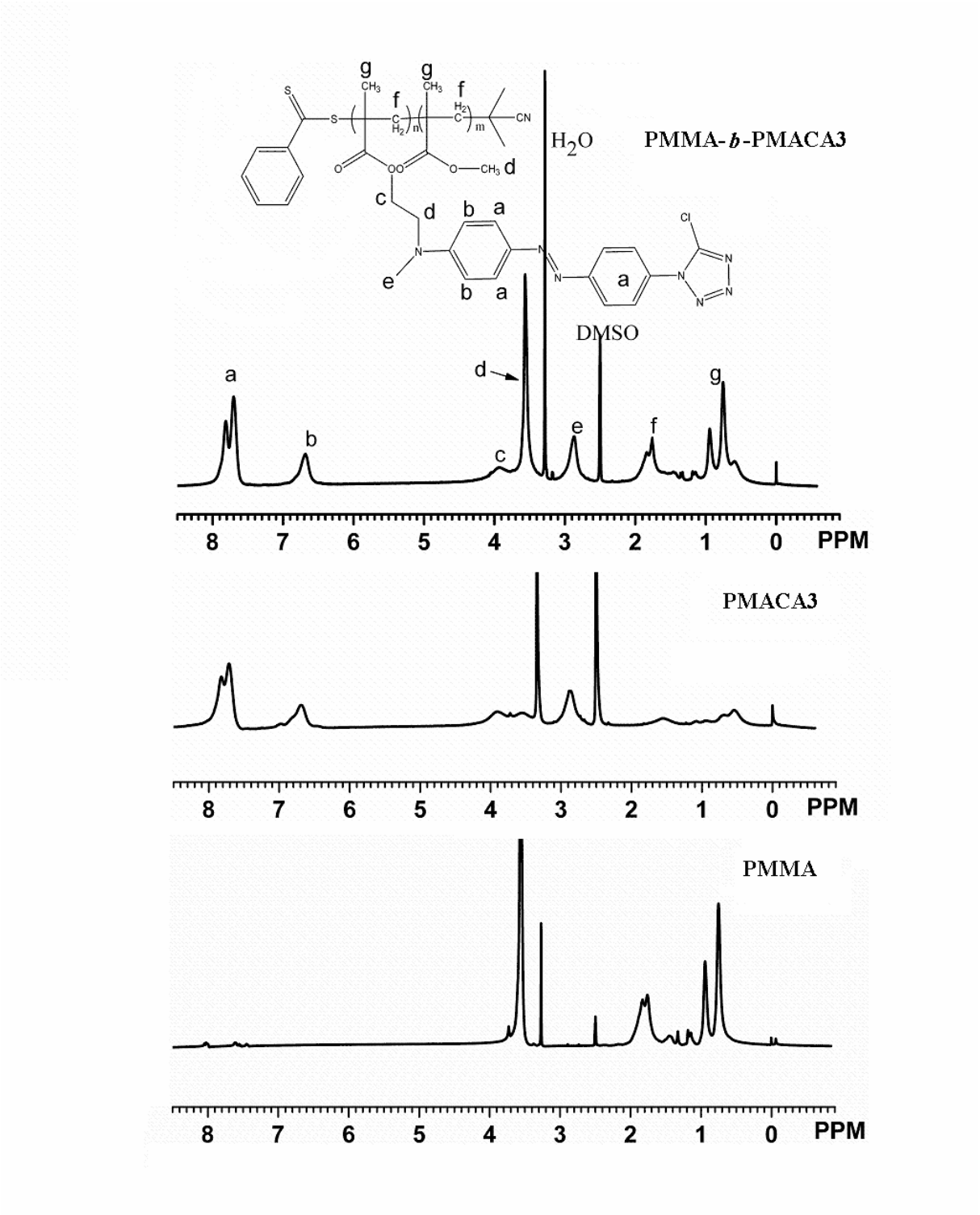

Figure 4

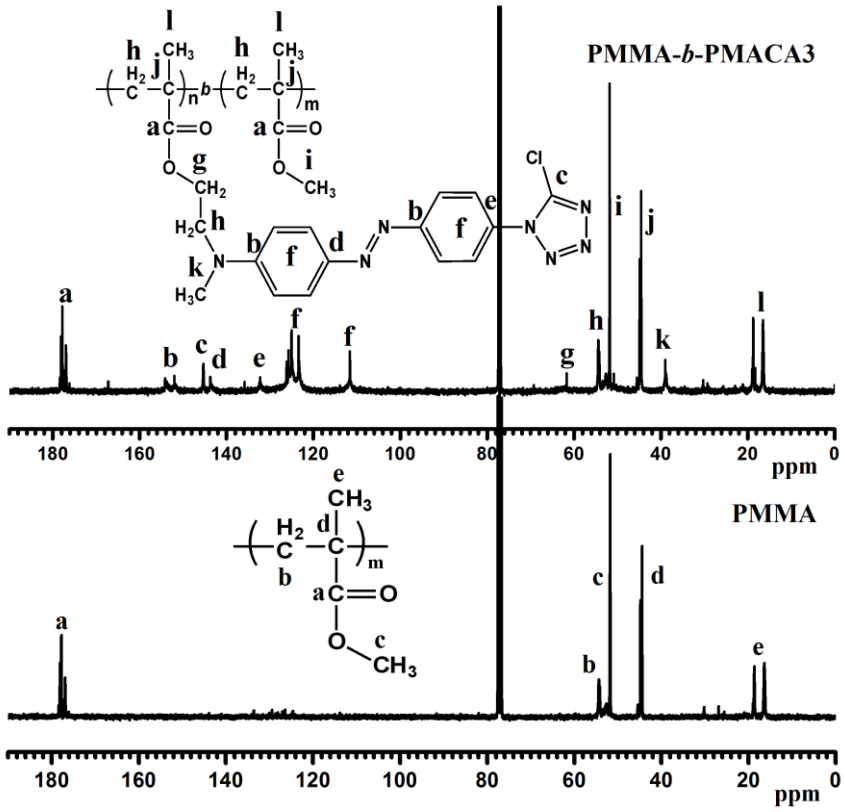

Figure 5

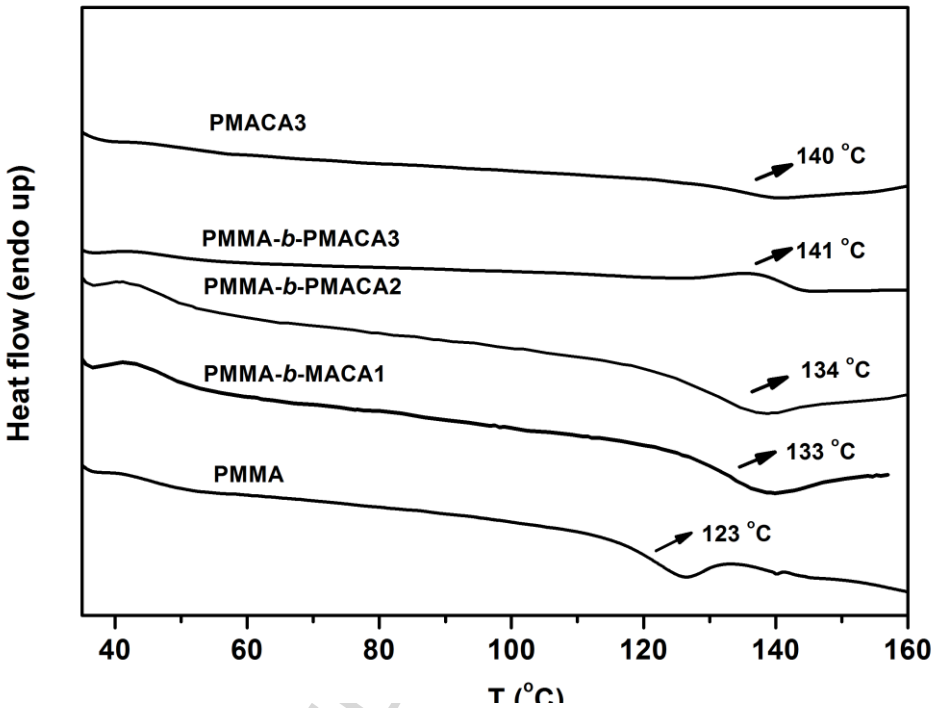

Figure 6

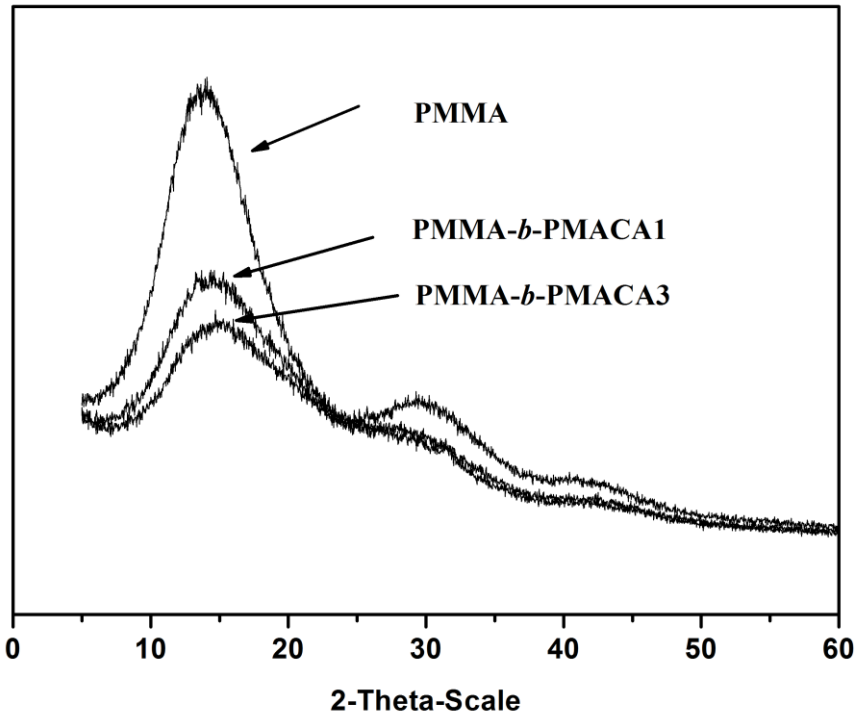

Figure 7

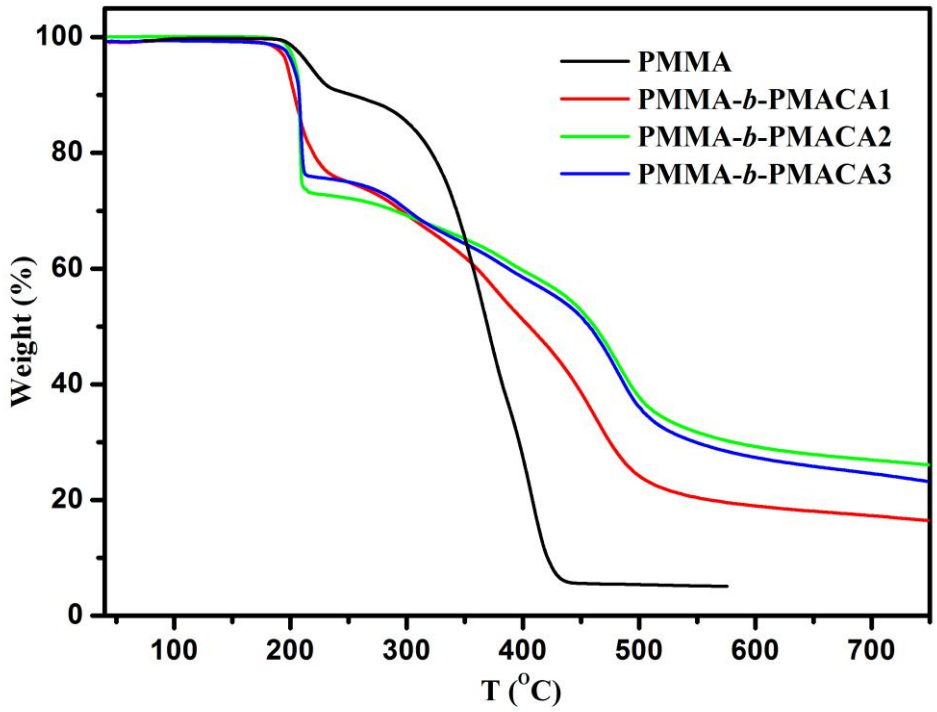

Figure 8

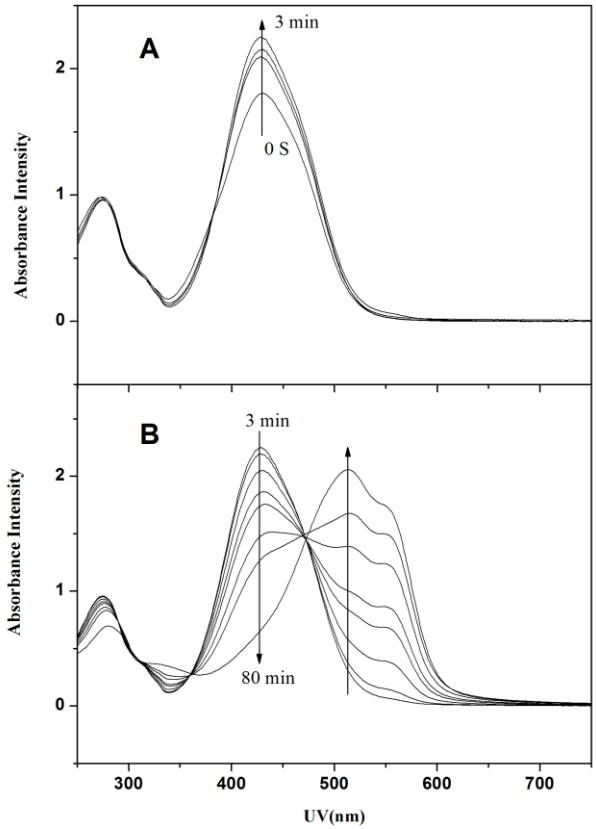

Figure 9

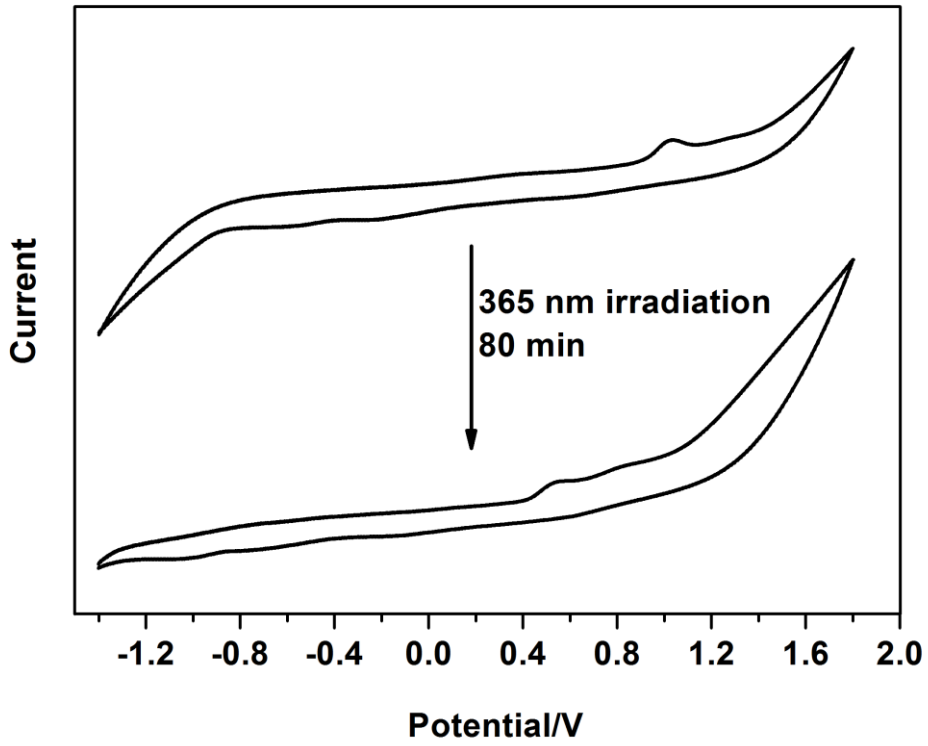

Figure 10

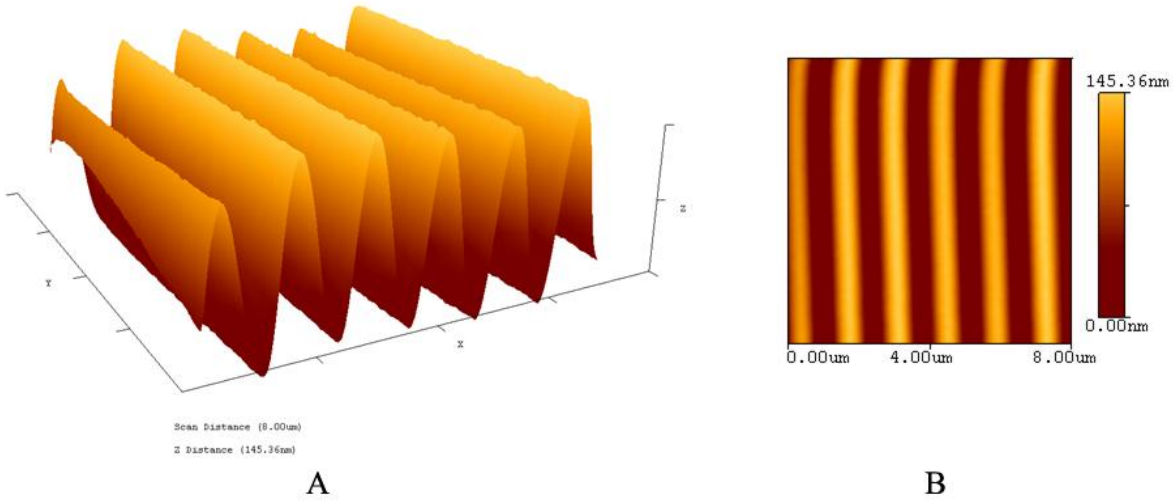

A B

Figure 11

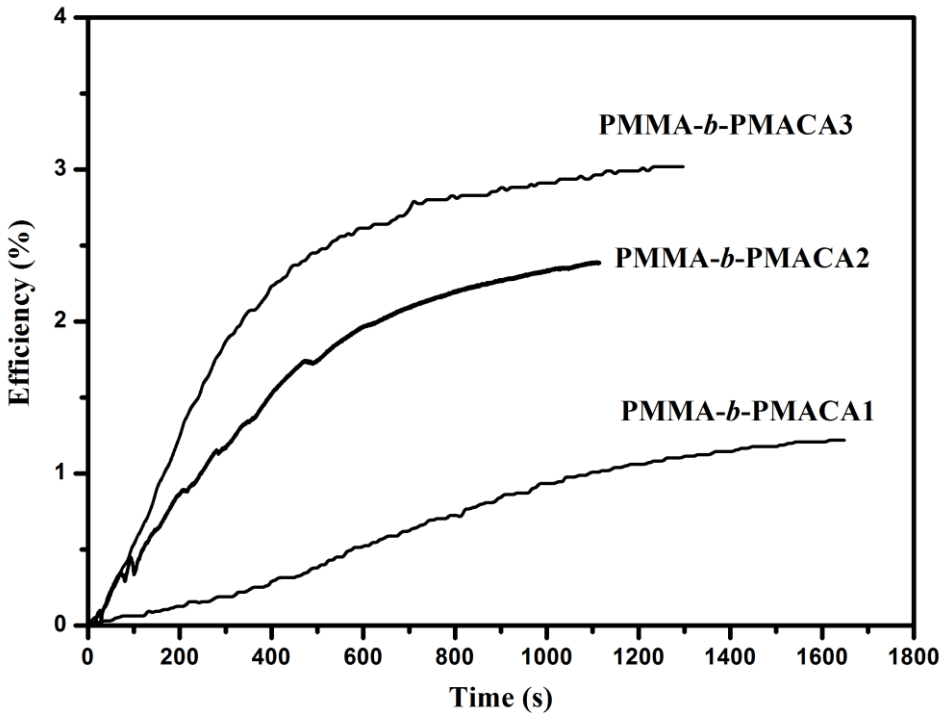

Figure 12

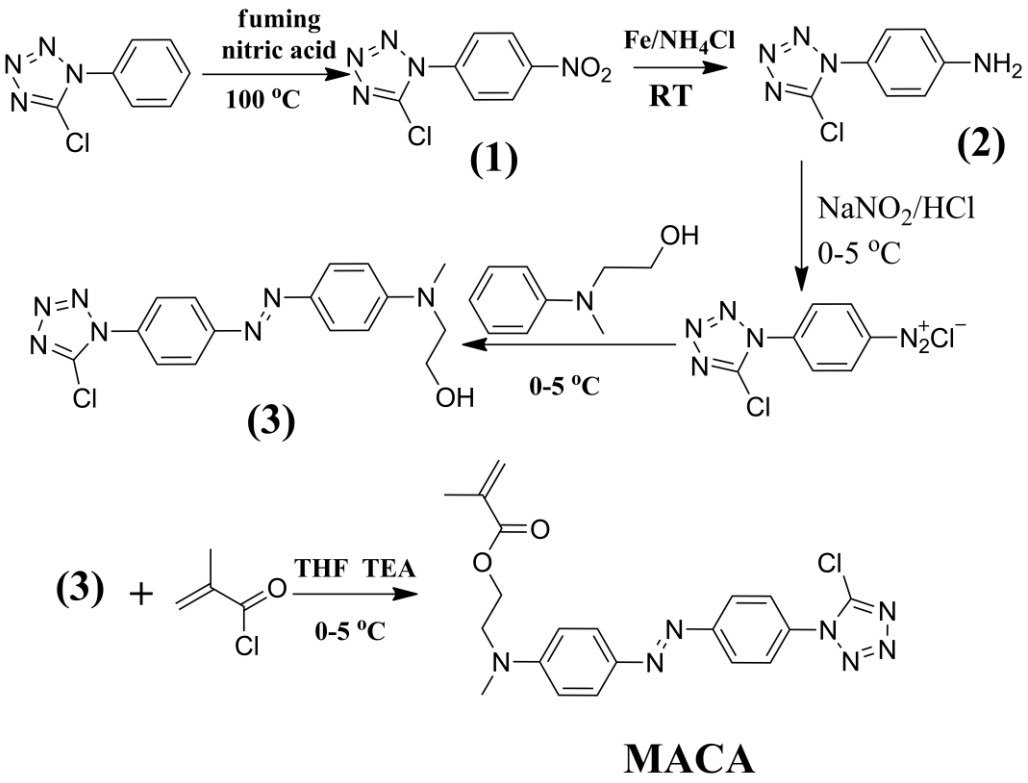

Scheme 1

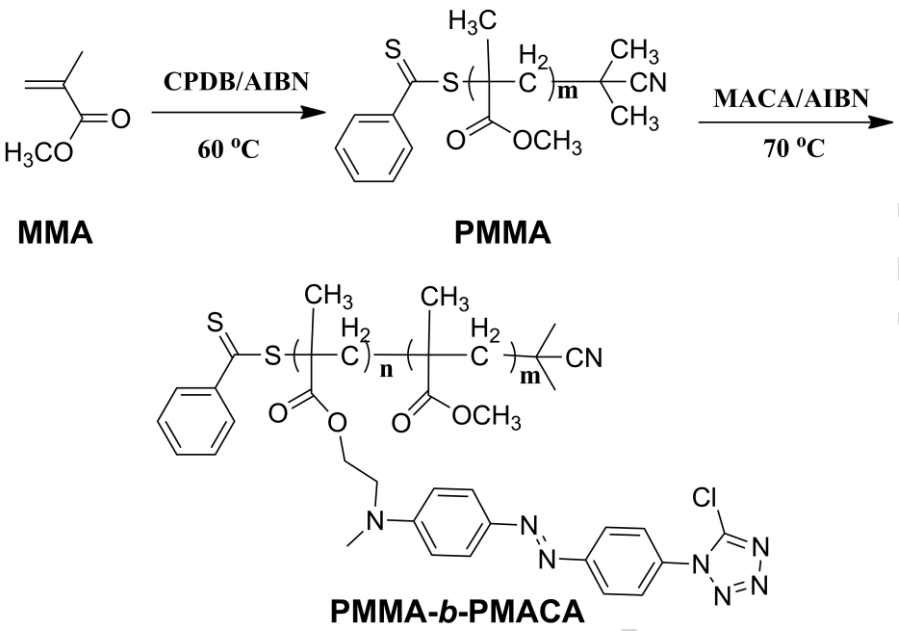

Scheme 2

Table 1. Characteristics of of PMMA, PMACAs and PMMA-*b*-PMACAs

Sample	Time (h)	*Conv.*[a)] (%)	$M_{n\,(GPC)}$[b)] (g/mol)	$M_{n\,(NMR)}$[b)] (g/mol)	$M_{n\,(th)}$[b)] (g/mol)	M_w/M_n
PMACA1	3	15.2	3800	-	2400	1.17
PMACA2	6	23.5	6400	-	5200	1.30
PMACA3	12	62.7	10200	-	13500	1.28
PMMA	12	83.1	8300	9100	7300	1.14
PMMA-*b*-PMACA1	6	18.7	12100	11400	12300	1.32
PMMA-*b*-PMACA2	9	36.4	15800	16500	16000	1.21
PMMA-*b*-PMACA3	24	51.6	19600	23400	19200	1.25

[a)] Conversion was determined by gravimetry.

[b)] $M_{n\,(GPC)}$, $M_{n\,(NMR)}$, $M_{n\,(th)}$: Molecular weight determined by GPC, ^{1}H NMR spectra, and theoretical molecular weight, respectively. $M_{n\,(th)}$ was calculated according to equation 1 for PMACA : $M_{n\,(th)} = [MACA]_0/[CPDB]_0 \times M_{MACA} \times \text{Conversion} + M_{CPDB}$, where $[MACA]_0$ and $[CPDB]_0$ were the initial concentration of $[MACA]_0$ and $[CPDB]_0$, respectively, M_{MACA} and M_{CPDB} were the molecular weight of MACA and CPDB, respectively; equation 2 for PMMA: $M_{n\,(th)} = [MMA]_0/[CPDB]_0 \times M_{MMA} \times \text{Conversion} + M_{CPDB}$; equation 3 for PMMA-*b*-PMACA: $M_{n\,(th)} = [MACA]_0/[PMMA]_0 \times M_{MACA} \times \text{Conversion} + M_{PMMA}$.